Original Article: Effects of Fourier Transform and Modal Theory in Electrotherapeutic Signals

Ebadollah Amouzad Mahdiraji

Department of Engineering, Sari Branch, Islamic Azad University, Sari, Iran

Use yor device to scan and read the article online

Citation E.A. Mahdiraji, **Effects of Fourier Transform and Modal Theory in Electrotherapeutic Signals,** *EJCMPR* . 2024; 3(1):1-6.

https://doi.org/10.5281/EJCMPR.20231110

Article info:
Received: **01 Jun 2023**
Accepted: **11 November 2023**
Available Online:
ID: EJCMPR-2311-1110
Checked for Plagiarism: **Yes**
Peer Reviewers Approved by:
Dr. Frank Rebout
Editor who Approved Publication:
Dr. Frank Rebout

Keywords:
Fault detection and localization indicators, power cables, short circuit fault, Fourier transform, Clarke transform, Modal components.

ABSTRACT

High and low voltage cables are among the most frequently utilized pieces of equipment in the power system and are subject to a variety of problems for a number of different causes. In spite of their increased reliability in airways, cables, whether power or distribution cables, are typically transported underground. As a result, they are more difficult to repair and may even need to be replaced in the event of a fault; for this reason, it is crucial to locate the fault as soon as possible. As is obvious from the research's title, the Fourier transform and modal transform methods are employed in this work to determine the kind and position of faults. This allows us to assess how effective the chosen method is at identifying and finding faults in subsurface infrastructure. The Fourier transform method, followed by the Modal transform, is anticipated to have a significant advantage in this study in terms of speed and accuracy when identifying the kind and location of defects. The nature and position of the defect are identified in the meanwhile using the detection and location indicators, which, according to simulations, will operate effectively. To show that these methods are accurate, the sample model is simulated. The exact and quick performance of the suggested strategy is confirmed by the simulation results from the MATLAB and EMTP/ATP software.

Introduction

According to the ANSI/IEEE Std. 100-1992 standard, a fault is a physical issue that prevents a device, component, or element from carrying out an essential function. This concept encompasses a short or clean wire termination. A short circuit between electrical phase conductors or between a phase and ground is almost always present in a fault. The problem could be a screw connection or there could be some impedance there. The aforementioned standards specify the term "fault," which is used as a synonym for "short circuit" [1]. The types of methods utilized to pinpoint the site of defects may vary depending on the defects that can arise in ground cables. Therefore, it is important to

***Corresponding Author: Ebadollah Amouzad Mahdiraji** (ebad.amouzad@gmail.com)*

first identify the type of defect that has occurred in the cable [2]. Online and offline techniques are the two main categories of approaches for locating cable faults. The cable failure is tested using specialized equipment in the offline technique whereas the fault spot is identified using voltage and current samples and processing in the online method [3]. In particular for the life-long power cables, a localization method based on the two ends of the cable is described [4]. The relative passivity coefficient changes as a result of cable aging, which also affects the positive, negative, and zero capacitors' capacitance [5]. The linear distribution model, the Clarke transform, and the discrete fourier transform (DFT) are all used in conjunction with the measurement of phasors from both ends of the cable to determine where the fault is [6]. In contrast to impedance-based techniques, a repeatable approach for fault location in cable is proposed in the reference [7]. The voltage and current equations are developed using sequential networks and the distributed parameter method to model the circuit. The fault distance is determined by applying the Newton-Raphson method. The technique is also applicable to cables with radial multi-sections and mild loads. The Allindar Dutch Network has been used in other works, which are shown in [8] and [9]. The computed reactance is all that fault locators use. In a realistic network model, short circuit scenarios are simulated in all nodes of a defective feeder because the fault impedance reactance is zero and the cable reactance is likewise specified and independent of the current. To determine the precise location, the computed impedance and the simulated impedance are compared. Within 5 minutes of the fault occurring, this method locates the distant site [10]. By modifying the energy held in the capacitor and inductor, which is produced on the lines or cables after the fault occurs, mobile waves can also be generated. In order to pass through the impedance discontinuities, both the voltage and the current waves travel along the circuit at a speed comparable to that of light. High frequency waves coming from the fault are then reflected and transmitted to the other. The fault distance is calculated using the product of the propagation velocity and the time interval of the fault, which is equal to the time interval between the instant of the wave-front's initial arrival and the instant the wave-front is reflected [11-14]. Nearly all methods based on mobile waves adhere to this principle. Introduces the fundamental locating principles as well as some convention finding techniques.

In this paper, a 230 kV transmission network with two sources at each end (representing a power network on each side) was first simulated in the EMTP/ATP transient states software, and then using the MATLAB software, the time outputs of this software are transmitted by transmitting the Fourier transform to Phasor domain. Eventually, the kind and location of the faults are identified utilizing the indications for fault localization and detection. The simulation results for various fault samples, various times, and various fault resistances are displayed in various figures and tables.

Fourier Transform

In general, Discrete Fourier Transform (DFT) is defined as follows [15]:

$$X(\omega) = \sum_{n=-\infty}^{\infty} x[n] e^{-i\omega n}$$

(1)

The above relation is considered as the main definition of the Fourier transform which is expressed in terms of discrete signals. If a signal is in a continuous form of x(t), in order to obtain a discrete Fourier transform, first a discrete signal x′(kΔt) is considered which includes N sample of the sampled signal x(t), the amount of which is expresses over time in relation (2):

$$x'(k\Delta T) = x(t)w(t)\sum_{k=-\infty}^{+\infty}\delta(t-k\Delta T)$$

(2)

Where ΔT is the sampling period and w(t) is the function that contains N sample of the sampled signal of x(t) at the time interval T_0, that is, this function can be introduced as a function with the sampling window to N length. For stable applications, the length of the sampling window is constant but this window moves forward over time and the samples from -∞ to ∞ enter and exit from the window, respectively and thus the sampling process is accomplished within time domain. Fourier transform of the sampled signal is expressed in the following relation, as defined in (3):

$$X'(f) = \sum_{k=-\infty}^{+\infty} a_k \delta(f - \frac{k}{T_0})$$

$$a_k = \frac{1}{T_0}\int_{-T_0/2}^{T_0/2}\left[\sum_{k=0}^{N-1} x(t)\times\delta(t-k\Delta T)\right]e^{-\frac{j\,2k\pi t}{T_0}}dt$$

(3)

Having simplified the formula (3) and considering NΔT= T_0, the relation of discrete Fourier transform is expressed as (4). Therefore, the discrete Fourier transform of the signal $x'(k\Delta t)$ will be as follows (5). But the general form of calculating the discrete Fourier transform that most of the authors use is as relation (6).

$$a_n = \sum_{k=0}^{N-1} x(k\Delta T)e^{\frac{-j\,2nk\pi}{N}} \qquad n = 0,\pm1,\pm2,\ldots$$

(4)

$$X'(\frac{n}{T_0}) = \sum_{k=0}^{N-1} x(k\Delta T)e^{\frac{-j\,2kn\pi}{N}} \qquad n = 0,1,2,\ldots N-1$$

(5)

$$X(r)\big|_{t=(r-1)\Delta T} = \frac{2}{N}\sum_{k=0}^{N-1} x(r+k)e^{-\frac{2\pi}{N}jk} \quad , \; r \geq 1$$

(6)

In the above relation, t=(r-1)ΔT is the Phasor time tag of the r^{th} sample. ΔT is equal to $1/f_s$, the distance between each two sampled signal. N is the number of the samples in each sampling cycle which is specified considering the sampling frequency (f_s) and power frequency (f) $N = \frac{f_s}{f}$. In the above relation, x(r+k) is also $r+k^{th}$ sample from the sampled signal of x(n). For example for the first Phasor x (1) calculated at zero time, it can be written in relation (7). It should be noted that the above relation is suitable for offline applications because it uses changes in subsequent samples in the calculation of Phasor and there is no delay in in following the signal changes. In real-time and immediate applications, the subsequent samples do not exist in waveform that can be used to calculate the Phasor, but the discrete Fourier transform algorithm from the previous samples to the former cycle is used, so there is a delay of NΔT seconds, unless the sampling window changes in accordance with sample variation. To adapt with the actual conditions, the Phasors obtained with the labels can be delayed by NΔT seconds or the relation (8) can be used for real time use:

$$X(1)\big|_{t=0} = \frac{2}{N}\sum_{k=0}^{N-1} x(1+k)e^{-j\frac{2\pi}{N}k} = \frac{2}{N}\left[x(1)e^{-j0} + x(2)e^{-j\frac{2\pi}{N}} + \ldots + x(N)e^{-j\frac{2\pi}{N}(N-1)}\right]$$

(7)

$$X(r)\big|_{t=(r-1)\Delta T} = \frac{2}{N}\sum_{k=0}^{N-1} x\left[(r-1+k-N)\Delta T\right]e^{-\frac{2\pi}{N}jk} \quad , \; r \geq 1$$

(8)

Clarke Transform

There is a significant electromagnetic coupling in the three-phase lines [16]. The phase domain signals are transformed into modal components using a modal transform in order to remove the coupling effect between phases and use the mobile wave approach. It is a well-known transformation that was applied in this essay. These quantities are independent, therefore any

calculation method is simple and unaffected by other calculation methods. Once this transformation has been used, the defect computation can be applied in any mode and the outcome can be based on it for analysis. In any event, this transformation will make the input of the three phase independent and can be applied to the three phase time waves and their phasors as well. As a result, different relations should be employed for the specified purpose in order to accomplish the goals of the problem since the Clarke transformation just conducts the transition from the fuzzy domain to the Modal [16]. For instance, some indications should be constructed based on the voltage and current relations in the modal domain and used to this end in this paper's short circuit calculations, identification of fault phases, and fault location [14].

Indicators of Fault Detection/ Localization

The Phasor measuring techniques are the foundation for the online fault identification and location for each three-phase line. On the basis of the equations stated in this section, the overall schematic of the comparative detecting/locating technique based on the Fourier transform is illustrated in Fig. 1.

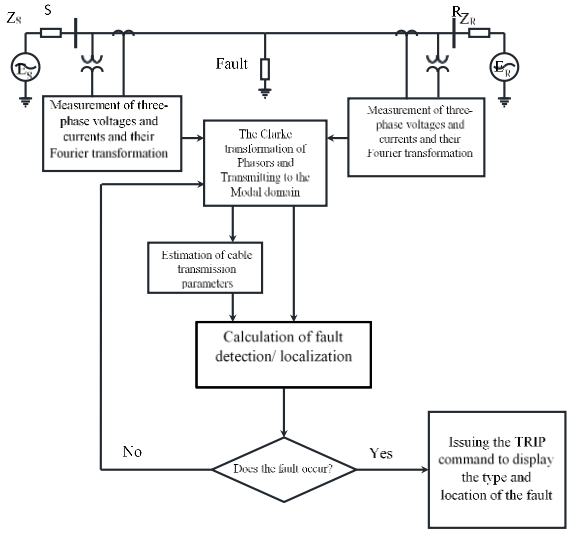

Figure (1). The structure of the comparative detecting/locating of EHV/UHV transmission line based on the Fourier and Modal Transformations and the defining indices.

The Simulation and Modeling of Cable Transmission Lines in the EMTP/ATP Software

For underground cables, the JMarti model is utilized in this work. Fig. (2) displays the analyzed model's single-line diagram. A voltage source of °10 230 and 230 kV is used to mimic the surrounding cable network on both sides of the S and R bus. Since the technique for employing the detection and location indicators is fully independent of the kind of network and depends on the phasor voltage and current at the two terminal ends linked to the cable, the features of the external networks and their modeling are not taken into account.

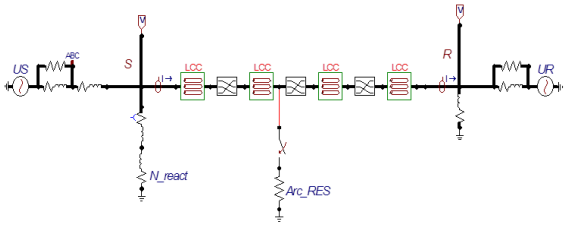

Figure (2). The single-line diagram and infinite bus

The cable between the two networks in the analyzed model has a 40-kilometer length and a 230kV rated voltage. Table (1) also displays the cable's physical features.

Table (1). The physical characteristics of XLPE cable with rated voltage of 230Kv

The parameter name	Value
Inner radius of core (cm)	0.0
Outer radius of core(cm)	2.34
Inner radius of pit (cm)	3.85
Outer radius of pit (cm)	4.13
External radius of insulation (cm)	4.84

Core resistance (Ω-m)	0.0170×10^{-8}
Insulation resistance (Ω-m)	0.2100×10^{-6}
ε_r for inner insulation	3.5
ε_r for outer insulation	8
Relative permeability coefficient μ_r	1.0
Ground resistance (Ω-m)	100

Comparison of the Results of Various Types of Faults

The relevant simulation of AG and BG single-phase faults and ABG two-phase fault for 1, 100, and 1000 ohm fault at 0.3 seconds and 0.305 seconds in various points of the cable at 50% and 25% cable length resistance at bus R is provided in the relevant tables in this section, along with information on the type and locations of the calculated faults as well as the time and calculation faults. It is also possible to calculate other faults at various times and locations, and the results can be shown.

The smallest defect is a short-circuit AG with a resistance of 1000 ohms at 0.3 seconds, or 0.0016%, or 41.5 milliseconds after an error occurs, or two power cycles. The completion of the Fourier transformation information window completion procedure is obviously tied to the delay of a cycle. Other than AG and ABG errors, an ohmic time of 0.305 seconds is seen significantly with rising error resistance, indicating that in addition to the detection time, the location time of the mistakes has also grown. In terms of error accuracy, the outcome is roughly the opposite, i.e., as error resistance grew, relative error accuracy likewise increased. As may be noted, the mistake is reduced with more time spent locating, and this is natural. It is simple to assess the efficacy of employing the combined strategy of this dissertation by observing and contrasting all the states listed in the table and their outcomes. The table above shows that, in the worst scenario, the gap between the computed erroneous position and the right location is 30 cm, or 36.9 meters, over a distance of 40 kilometers.

The 1000-ohm single-phase fault at 0.305 seconds is related to the lowest fault of 0.9 ms and the largest fault of 18.8 ms. The locating indicator's lowest fault is calculated at 0.009%, which is equal to a longitudinal fault of 2.7 cm per 40 km. On the other hand, the fault of this indication is 0.1231%, or 36.9 meters, and it emerges at 0.305 seconds in the ABG two-phase fault with a 1-ohm resistor. In terms of location time, the smallest location fault is connected to the AG fault of 100 ohms at 0.3 seconds with a location fault of 0.0117%, or 32.6 milliseconds, and the highest location fault is related to the AG fault of 0.305 seconds with a location fault of 163.9 milliseconds, as in the previous condition. Although the size of the locational fault is based on the percentage of comparison and is significant, the absolute determined values must also be calculated on the basis of the short line's length, which is not specified in the reference articles. Table (2) makes it evident that the short-circuit placement fault in this thesis is much lower than in references [12–14] and illustrates how the method suggested in this study is better than other ways like the wavelet transform. The length of the cable as well as the nature and timing of the problem are not mentioned in this reference.

Table (2). Evaluation of the proposed method than other methods

Method	The percent of fault	The fault location
Wavelet transform	4.48	512
Fit curve	3.36	508
The proposed method of the article	3.26	506

Conclusion

In this study, a powerful method for determining the size and angle of each phase is provided. This method provides complete details on the voltage parameters and power grid flows. The good performance of an online method using detection and location indicators in both the modal and fuzzy domains is demonstrated using Fourier transform data on both sides of a cable connection. It has been suggested to use Clarke transformation and transition to the modal domain for the independence of the components used to study a variety of studies, including fault. This method not only reduces the volume of equations caused by the dependence between fuzzy components, but also increases the degree of assurance of the accuracy of the results. The Fourier transform calculations are the only thing that add any significant delay to the problem detection and location indicators. Additionally, the computations of these indicators are fairly accurate, and in this instance, the main error lies in the Fourier transformation's fundamental design. Fault detection indicators' answers in the modal and even fuzzy domains are also always accurate. The largest computational error in the modal domain brought on by the fault location indicator was less than 5.0%. The proposed hybrid approach's precision extends beyond a few techniques, such the wavelet transform.

References

[1] A Fathi, et al., International Journal of Adhesion and Adhesives, **2023**, 122, 103322 [Crossref], [Google Scholar], [Publisher]

[2] E Ghasemi, AH Fathi, S Parvizinia., J Iran Dent Assoc **2019**; 31 (3):169-176 [Crossref], [Google Scholar], [Publisher]

[3] HQ. Alijani, A. Fathi, et al. Bioref. **2022**. [Crossref], [Google Scholar], [Publisher]

[4] M Maalekipour, M Safari, M Barekatain, A Fathi, International Journal of Dentistry, **2021**, Article ID 3178536, [Crossref], [Google Scholar], [Publisher]

[5] A Fathi, Ebadian, S Nasrollahi Dezaki, N Mardasi, R Mosharraf, S Isler, S Sadat Tabatabaei, " International Journal of Dentistry, vol. 2022, Article ID 4748291, 10 pages, 2022. [Crossref], [Google Scholar], [Publisher]

[6] A. Fathi, et al., Dent Res J (Isfahan). **2023** 18; 20: 3. [Google Scholar], [Publisher]

[7] A.H Fathi; S. Aryanezhad; E Mostajeran; U Zamani Ahari; S.M Asadinejad. The Iranian Journal of Obstetrics, Gynecology and Infertility, **2022**, 25(2), 90-100. [Crossref], [Google Scholar], [Publisher]

[8] B. Ebadian, A Fathi, Sh Tabatabaei, International Journal of Dentistry, **2023**, Article ID 3347197, 15 [Crossref], [Google Scholar], [Publisher]